

# Electrical and optical anisotropic properties of rhenium-doped molybdenum disulphide

K.K. Tiong<sup>a,\*</sup>, Y.S. Huang<sup>b</sup>, C.H. Ho<sup>c</sup>

<sup>a</sup>Department of Electrical Engineering, National Taiwan Ocean University, Keelung 202, Taiwan, ROC

<sup>b</sup>Department of Electronic Engineering, National Taiwan University of Science and Technology, Taipei 106, Taiwan, ROC

<sup>c</sup>Department of Electronic Engineering, Kuang Wu Institute of Technology and Commerce, Peitou, Taipei 112, Taiwan, ROC

## Abstract

Single crystals of rhenium (Re)-doped MoS<sub>2</sub> have been grown by chemical vapor transport method using bromine as a transport agent. Single crystalline platelets up to 10×10 mm<sup>2</sup> surface area and 2 mm in thickness are obtained. By analyzing the X-ray diffraction profile, the structure of the single crystals shows rhombohedral symmetry. The Hall measurements indicate that the samples are n-type in nature. The thicker Re-doped MoS<sub>2</sub> samples enable easier exploration of the electrical and optical anisotropies of the materials both parallel and perpendicular to the *c* axis of the crystals. The anisotropy of electrical conductivity perpendicular to and along the *c* axis for the Re-doped MoS<sub>2</sub> is about 10<sup>2</sup> and is at least one order smaller than 10<sup>3</sup> for the undoped samples. The optical anisotropic property was studied using electrolyte electroreflectance measurements. The excitonic transitions of A and B features parallel to *c* axis show different degrees of red shift in comparing with the features perpendicular to *c* axis and with that of the undoped sample. The role of rhenium in affecting both the electrical and optical properties of the MoS<sub>2</sub> crystals is examined. © 2001 Elsevier Science B.V. All rights reserved.

**Keywords:** Rhenium-doped molybdenum disulphide; Anisotropic properties

## 1. Introduction

Molybdenum disulphide belongs to the group VIA transition metal dichalcogenides MX<sub>2</sub> where M=Mo or W and X=S or Se [1,2]. These layered structure transition metal dichalcogenides have been of considerable interest because of their extreme anisotropic electrical, optical and mechanical properties [1–4]. MoS<sub>2</sub> has always been used as a prototype for the study of the family group and is of particular interest because of the resource abundance of the naturally occurring molybdenite and also the possible occurrence of two polytypes of the material [5]. These two known modifications are termed 2H- and 3R-MoS<sub>2</sub>. In the 2H-polytype, two layers per unit cell are stacked in hexagonal symmetry and the structure belongs to the space group *D*<sub>6h</sub><sup>4</sup>. The 3R-modification has three layers along the *c* direction stacked with rhombohedral symmetry and belongs to the space group *C*<sub>3v</sub><sup>5</sup>. The intralayer bonding is thought to be predominantly covalent while the interlayer bonding is of the weak van der Waals type [1,2,6]. Earlier works suggested that the rhombohedral modification is metastable and converts to the hexagonal form by brief

heating at 600°C and higher temperature for ~22 days [5]. However from the more recent work, 3R-MoS<sub>2</sub> have been synthesized from stoichiometric proportions of the component elements at a significantly higher temperature over 900°C by incorporating a small amount of rhenium during growth [7]. The as-grown rhenium (Re)-doped MoS<sub>2</sub> possesses a large and smooth surface normal to *c* axis with an area up to 10×10 mm and a thickness of 2 mm along the *c* direction. The larger surface areas perpendicular (van der Waals plane) and parallel (edge plane) to the *c* axis enable easier exploration of the electrical and optical anisotropic properties of the crystals which are thus far difficult to achieve due to the relatively thin 2H- or undoped MoS<sub>2</sub> [3].

In this work, we report on the growth and characterization of Re-doped MoS<sub>2</sub> crystals prepared by chemical vapour transport method with bromine as a transport agent. Undoped MoS<sub>2</sub> has also been grown for the purpose of comparison. The structural analysis was also carried out with the help of X-ray diffractometry. The temperature-dependent electrical conductivity and Hall coefficient were measured between 20 and 300 K using the van der Pauw technique along and perpendicular to the *c* axis for the determination of the crystal's electrical anisotropy. Optical anisotropy of the excitonic transitions A and B was also

\*Corresponding author.

E-mail address: kktiong@ind.ntou.edu.tw (K.K. Tiong).

studied using the electrolyte electroreflectance (EER) measurement. The role of rhenium in affecting the variation of the red shifts of A and B excitons for both parallel and perpendicular  $c$  axis directions for the Re-doped  $\text{MoS}_2$  will be examined.

## 2. Crystal growth

Both undoped and Re-doped  $\text{MoS}_2$  single crystals were grown using chemical vapor transport method with  $\text{Br}_2$  as a transport agent. A total charge of 10 g, which consisted of stoichiometric composition of the constituent elements and dopant were used in each growth experiment. Prior to the crystal growth, a quartz ampoule (20 cm length  $\times$  22 mm O.D.  $\times$  17 mm I.D.) containing  $\text{Br}_2$  ( $\sim 5 \text{ mg/cm}^3$ ) and the elements (Mo, 99.99% pure; Re, 99.99%; S, 99.999%) was cooled with liquid nitrogen, evacuated to  $10^{-6}$  Torr and sealed. It was shaken well for uniform mixing of the powder. The ampoule was placed in a three-zone furnace and the charge prereacted for 24 h at  $800^\circ\text{C}$  with the growth zone at  $950^\circ\text{C}$ , preventing the transport of the product. The temperature of the furnace was increased slowly to avoid any possibility of explosion due to the exothermic reaction between the elements. The furnace was then equilibrated to give a constant temperature across the reaction tube, and programmed over 24 h to produce the temperature gradient at which single-crystal growth took place. Optimal results were obtained with temperature gradient of approximately  $960 \rightarrow 930^\circ\text{C}$ . After 240 h, the furnace was allowed to cool down slowly ( $40^\circ\text{C/h}$ ) to about  $200^\circ\text{C}$ . The ampoule was then removed and wet tissues applied rapidly to the end away from the crystals to condense the  $\text{Br}_2$  vapor. When the ampoule reached room temperature, it was opened and the crystals removed. The crystals were then rinsed with acetone and deionized water. Single crystalline platelets up to  $10 \times 10 \text{ mm}^2$  surface area and 2 mm in thickness were obtained. The as-grown rhenium-doped  $\text{MoS}_2$  single crystal is shown in Fig. 1.  $\text{MoS}_2$  crystallizes with 2H or 3R structure, while  $\text{ReS}_2$  crystallizes in a distorted C6 structure [1], so that we do not expect the two solid solutions to be miscible. It was found that a 5% nominal doping of  $\text{MoS}_2$  prevented the growth of single crystals [7].

The rhenium composition was estimated by energy dispersive X-ray analysis (EDX). A considerable discrepancy exists between the nominal doping ratios and those determined by EDX. The nominal concentration is estimated to be much larger than the actual one. Because no Re could be detected in EDX even though this method is sensitive for concentrations  $\geq 1\%$  [8], we conclude that Mo and Re metals are most likely be chemically transported at different rates and most of the doping material must remain in the 'untransported' residual charge. For the experiments, the concentration of rhenium is taken to be the nominal starting composition.



Fig. 1. Photograph of the as-grown Re-doped  $\text{MoS}_2$  crystal showing the prominent van der Waals surface.

## 3. Experiments

### 3.1. X-ray diffraction

Several small crystals from samples of as grown undoped  $\text{MoS}_2$  and Re-doped  $\text{MoS}_2$  with nominal rhenium concentrations of 0.5 and 1% were finely ground with a mixture of glass powder. The X-ray powder patterns (not shown) were taken and recorded by means of a slow moving radiation detector.  $\text{CuK}_\alpha$  radiation was employed and a silicon standard was used to calibrate the diffractometer. Lattice parameters were calculated with the aid of a computer using a least-squares refinement program.

The X-ray patterns of the Re-doped  $\text{MoS}_2$  crystals show the presence of additional lines which are determined to be due to the formation of the rhombohedral polytype having cell dimensions  $a = 3.164 \text{ \AA}$  and  $c = 18.371 \text{ \AA}$ . For the undoped  $\text{MoS}_2$ , a hexagonal lattice structure is obtained with cell dimensions evaluated to be  $a = 3.160 \text{ \AA}$  and  $c = 12.295 \text{ \AA}$ .

### 3.2. Conductivity and Hall measurements

The electrical properties of Re-doped  $\text{MoS}_2$  were studied by measuring the conductivity and Hall coefficient along and perpendicular to the crystal's  $c$  axis. The measurements were performed between 20 and 300 K using the van der Pauw technique. Contacts were made with silver paint. For comparison, similar measurements were also carried out for the undoped  $\text{MoS}_2$  perpendicular to the  $c$  axis. Hall measurements revealed n-type semiconducting behaviour for both the undoped and Re-doped  $\text{MoS}_2$ . From Fig. 2, one can see that the conductivity increases significantly with Re concentration, which indicates increasing number of charge carriers available for conduction. The extra electrons of the Re ions must have provided for the increase in conductivity. The anisotropy

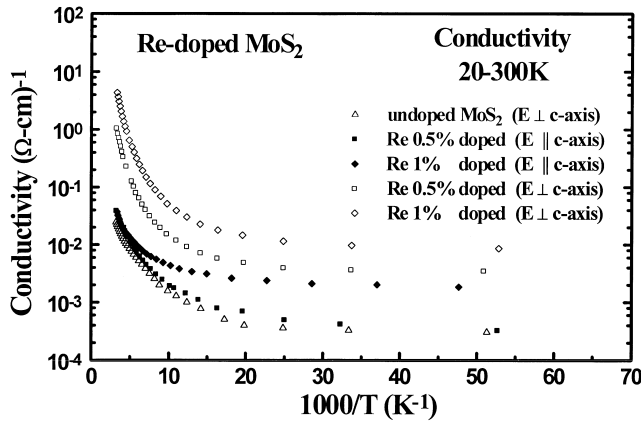


Fig. 2. Temperature dependent anisotropic conductivity for the Re-doped  $\text{MoS}_2$  in the range 20–300 K. Undoped  $\text{MoS}_2$  is included for comparison.

of the conductivity perpendicular to and along the  $c$  axis is evaluated to be  $10^2$  for the Re-doped samples which is an order smaller than  $10^3$  for the undoped  $\text{MoS}_2$  (not shown). This trend is similar to the anisotropy of Re-doped  $\text{MoSe}_2$  (30) as compared to undoped sample ( $10^4$ ) [8]. From the temperature dependences of the Hall coefficient and conductivity, the carrier concentrations  $n = 1/|eR_H|$  (not shown) and the Hall mobility  $\mu_H$  (as shown in Fig. 3) in the basal plane were determined. The carrier concentration evaluated from the Hall measurement is similar to the conductivity measurement in which a marked increase with Re concentration is recorded. The Hall mobility in Fig. 3 increases with increasing temperature over the range 20 to 150–170 K. This is a characteristic of the dominant impurity scattering. Above 150–170 K, the mobility decreases with increasing temperature up to 300 K, which corresponds to the region where electron-phonon scattering is dominant. In general, the mobility of the doped samples is smaller than the undoped one. It is also noticed that our measured values vary somewhat from crystal to crystal

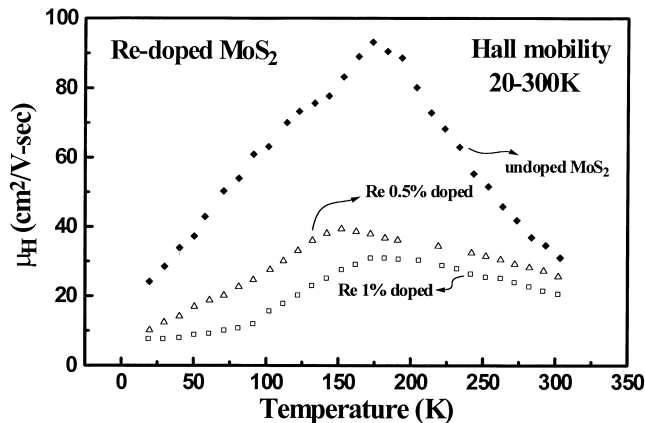


Fig. 3. Temperature dependent Hall mobility of the Re-doped and undoped  $\text{MoS}_2$  in the range 20–300 K.

even when taken from the same batch. Such differences are most likely due to the actual uncontrollable doping concentrations or nonstoichiometry of the crystals.

### 3.3. Electrolyte electroreflectance measurements

For the EER experiment, maximum size crystals of 1% Re-doped  $\text{MoS}_2$  were selected. The EER were taken on a fully computerized set-up for modulation spectroscopy described elsewhere [9]. Detailed investigations of the polarization dependence of the prominent features, A and B excitons in the energy range 1.75–2.25 eV were undertaken and illustrated in Fig. 4. For the Re-doped  $\text{MoS}_2$ , the spectra were recorded for the perpendicular ( $E \perp c$ ) and parallel ( $E \parallel c$ ) polarizations together with an unpolarized spectrum for the  $k \perp c$  (edge plane) configuration while only the  $E \perp c$  spectrum was recorded for the  $k \parallel c$  (van der Waals plane) configuration. For the undoped  $\text{MoS}_2$ , only the  $k \parallel c$ ,  $E \perp c$  spectrum was recorded.

The experimental curves in Fig. 4 have been fitted to a Lorentzian line shape function of the form [9,10]

$$\frac{\Delta R}{R} = \text{Re} \sum_{i=1}^m C_i e^{j\phi_i} [E - E_i + j\Gamma_i]^{-2} \quad (1)$$

where  $C_i$  and  $\phi_i$  are the amplitude and phase of the lineshape,  $E_i$  and  $\Gamma_i$  are the energy and linewidth of the interband transition. The fits yield the parameters  $C_i$ ,  $E_i$  and  $\Gamma_i$ . The least square fits using Eq. (1) are shown as solid curves in Fig. 4.

The EER spectrum for the undoped  $\text{MoS}_2$  is displayed on the bottom of Fig. 4. For exciton A, two bands,  $E_{A_1} = 1.881$  eV and  $E_{A_2} = 1.925$  eV were detected. The direct band gap  $E_g = 1.94$  eV and the exciton binding energy  $R = 58.7$  meV can be estimated [2,11]. These values are similar to those of Ref. [2]. The broad shoulders located at 1.986 eV ( $\text{AR}_A$ ) and 2.15 eV ( $\text{AR}_B$ ) are similar

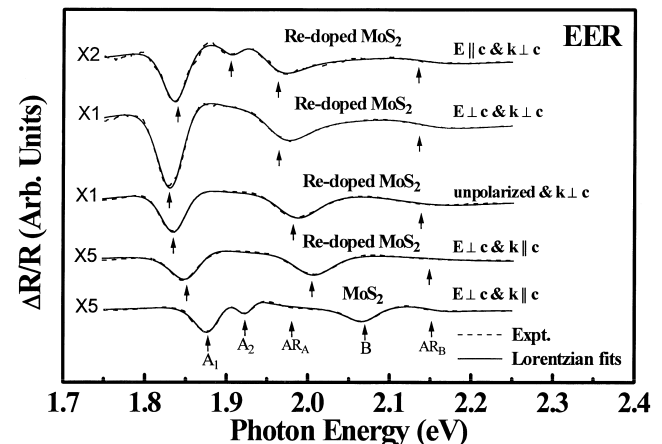


Fig. 4. Polarized EER spectra of Re-doped  $\text{MoS}_2$  with  $k \perp c$  and  $k \parallel c$  configurations. For undoped  $\text{MoS}_2$  only the  $k \parallel c$  spectrum is performed.

and are identified to be the antiresonance structures [2]. For exciton B, a probable mixing of  $n=1$  band with higher bands results in a much broader feature being detected at 2.07 eV.

The EER spectra for the 1% Re-doped  $\text{MoS}_2$  sample are displayed at the top of Fig. 4. A most noticeable difference is the absence of higher bands for all the spectra of Re-doped  $\text{MoS}_2$ . The energy location of excitons A and B are red-shifted for the Re-doped  $\text{MoS}_2$ . In particular, the red shift of 65 meV for exciton B for the  $k\parallel c$  configuration is identical with the separation of the feature labeled as  $B^*$  from exciton B of the WMR measurement of Ref. [12] where the same  $k\parallel c$  configuration is being employed. The presence of  $B^*$  is attributed to the coexistence of 3R and 2H phases [5,12] in their synthetic crystals. In this work, the ‘purity’ of the recorded spectra indicates the good quality of our samples. In the case of Re-doped  $\text{MoS}_2$ , exciton A appeared sharper while exciton B appeared much broader than that of the undoped sample. This is most likely a consequence of superposition of the red shifted exciton B and the broad antiresonance feature  $AR_A$  [13]. In the  $k\perp c$ ,  $E\parallel c$  spectrum, we have also detected a distinct structure of unknown origin located in between excitons A and B at 1.906 eV.

In the following, the focus of our discussion is on the different physical mechanisms affecting the measured red shifts of excitons A and B. A comparison of the spectra of  $k\parallel c$  configuration for the undoped and Re-doped  $\text{MoS}_2$  in Fig. 4 show that excitons A and B for Re-doped  $\text{MoS}_2$  are red shifted by 27 and 65 meV, respectively. The observed red shifts can be accounted for qualitatively by the change in crystal symmetry due to presence of rhenium impurity. During growth of the doped samples, the rhenium ions can either substitute part of the Mo atoms in the  $\text{MoS}_2$  lattice [5,7] or intercalate between the van der Waals gaps. From the results of our previous study [14] it is most probably the latter process which predominates and results in the formation of 3R- $\text{MoS}_2$ . Consequently, the electronic states of the materials are perturbed together with the interlayer interactions. This effect results in the red shift of the excitonic transitions with the energy separation of the spin orbit doublet reduced from 189 meV for undoped  $\text{MoS}_2$  to 151 meV for Re-doped  $\text{MoS}_2$ . The values for energy separation of exciton doublets agree well with the literature and are quite temperature insensitive [2,12,14,15].

From Fig. 4, for Re-doped  $\text{MoS}_2$ , the spectra of  $k\parallel c$  and  $k\perp c$  configurations with  $E\perp c$  polarization showed the measured difference for the peak positions of excitons A and B to be identical and equal to 21 meV. The measured difference is being attributed to the crystal anisotropy [16,17]. A qualitative understanding of crystal anisotropy can be realized as follows. The ground state excitonic transition in Re-doped (3R-)  $\text{MoS}_2$  can be described by a two-dimensional Mott–Wannier [11,18] hydrogen-like series  $E_1 = E_g - R^*$ , where  $E_g$  is the band gap and  $R^*$  is the effective Rydberg constant [17,18] which is propor-

tional to  $\mu/\epsilon^2$ . The parameter  $\mu$  is the effective mass of the exciton and  $\epsilon$  is the dielectric constant of  $\text{MoS}_2$ . Crystal anisotropy has been shown to affect the exciton effective mass and the crystal dielectric constant parallel and perpendicular to the crystal  $c$  axis. For  $\text{MoS}_2$ , we have  $\epsilon_{\perp} > \epsilon_{\parallel}$  and  $\mu_{\parallel} > \mu_{\perp}$  [12,19]. The band gap of the layered structure is also affected by the crystal anisotropy with  $E_{g\parallel} > E_{g\perp}$  [16]. The resulting induced red shift for the ground state can then be qualitatively given by  $\Delta E = E_{1\parallel} - E_{1\perp} = E_{g\parallel} - E_{g\perp} + R_{\perp}^* - R_{\parallel}^*$ . The measured crystal anisotropy induced red shift of 21 meV for Re- $\text{MoS}_2$  is about twice as large as those of  $\text{WSe}_2$  by Chaparro et al. [16].

The spectra from the edge plane surface ( $k\perp c$ ) with  $E\perp c$  and  $E\parallel c$  polarizations showed energy of exciton A at 1.833 and 1.838 eV, respectively. The broader exciton B is insensitive to this polarization. The measured shift of 5 meV though small is consistent by careful repetition of the experimentally recorded  $E\parallel c$  and  $E\perp c$  spectra. It was also found that the recorded unpolarized spectrum can be obtained by taking an ‘average’ of the two spectra with orthogonal polarization resulting in the ‘average’ peak position of exciton A at 1.836 eV. The physical origin of this shift may come from another source. The intralayer bonding is part ionic and part covalent with the latter being dominant [6,20]. The presence of Re atoms in the  $\text{MoS}_2$  lattice has the effect of enhancing the ionicity of the metal–chalcogen bonding resulting in an increase of the lattice polarizability [6] of the Re-doped  $\text{MoS}_2$ . The lattice field interacting effect is much more pronounced for electric field perpendicular to the  $c$  axis than parallel to it and results in a shift of 5 meV in exciton A. The relatively weak effect is most likely due to the nature of the intralayer bonding of the  $\text{MoS}_2$  lattice, which is predominantly covalent.

#### 4. Summary

In summary, we have measured the temperature dependence of the electrical conductivity and the polarization dependence of EER for both undoped and Re-doped  $\text{MoS}_2$  samples. The presence of rhenium impurity has been determined to play a major role in influencing electrical and optical properties of the doped samples. The Re ions intercalate between the van der Waals gaps of the 2H- $\text{MoS}_2$  lattice resulting in the formation of 3R- $\text{MoS}_2$ . The electrical anisotropy of the doped sample is reduced by a factor of  $10-10^2$ . From the EER measurements, the energy separation of the exciton doublets has been found to reduce from 189 meV for the undoped  $\text{MoS}_2$  to 151 meV for the doped sample. The crystal anisotropy induced red shift for the doublets are identical and equal to 21 meV. Our works also point to the possible effect of intralayer lattice field on the experimental data.

## Acknowledgements

This work is supported by the National Science Council of the Republic of China under project numbers NSC 89-2112-M-019-002 and NSC 89-2112-M-011-001.

## References

- [1] J.A. Wilson, A.D. Yoffe, *Adv. Phys.* 18 (1969) 193.
- [2] A.R. Beal, J.C. Knights, W.Y. Liang, *J. Phys. C: Solid State Phys.* 5 (1972) 3540.
- [3] W.Y. Liang, *J. Phys. C: Solid State Phys.* 6 (1973) 551.
- [4] J.A. Ogilvy, *Wear* 160 (1993) 171.
- [5] A.N. Zelikman, G.V. Indenbaum, M.V. Teslitskaya, V.P. Shalankova, *Soviet Phys. -Crystallogr.* 14 (1970) 687.
- [6] G. Weiser, *Surface Sci.* 37 (1973) 175.
- [7] K.K. Tiong, P.C. Liao, C.H. Ho, Y.S. Huang, *J. Cryst. Growth* 205 (1999) 543.
- [8] M.K. Agarwal, P.D. Patel, S.K. Gupta, *J. Cryst. Growth* 129 (1993) 559.
- [9] D.E. Aspnes, in: M. Balkanski (Ed.), *Handbook On Semiconductors*, Vol. 2, North-Holland, Amsterdam, 1980, p. 109.
- [10] F.H. Pollak, H. Shen, *Mater. Sci. Eng. R10* (1993) 275.
- [11] A.R. Beal, W.Y. Liang, *J. Phys. C: Solid State Phys.* 9 (1976) 2459.
- [12] E. Fortin, F. Raga, *Phys. Rev. B* 11 (1975) 905.
- [13] K.K. Tiong, T.S. Shou, *J. Phys.: Condens. Matter* 12 (2000) 5043.
- [14] K.K. Tiong, T.S. Shou, C.H. Ho, *J. Phys.: Condens. Matter* 12 (2000) 3441.
- [15] C.H. Ho, C.S. Wu, Y.S. Huang, P.C. Liao, K.K. Tiong, *J. Phys.: Condens. Matter* 10 (1998) 9317.
- [16] A.M. Chaparro, P. Salvador, B. Coll, M. Gonzalez, *Surface Sci.* 293 (1993) 881.
- [17] P.Y. Yu, M. Cardona, in: *Fundamentals of Semiconductors*, Springer-Verlag, 1996, p. 266.
- [18] S.L. Chuang, in: J.W. Goodman (Ed.), *Physics of Optoelectronic Devices*, Wiley, 1995, p. 102.
- [19] R. Coehoorn, C. Haas, R.A. de Groot, *Phys. Rev. B* 35 (1987) 6203.
- [20] A.R. Beal, H.P. Hughes, *J. Phys. C: Solid State Phys.* 12 (1979) 88.